Ploidy level enhances the photosynthetic capacity of a tetraploid variety of *Acer buergerianum* Miq.

Yi Wang [Equal first author, 1, 2] , **Bingyu Jia** [Equal first author, 1, 3] , **Hongjian Ren** [4] , **Zhen Feng** [Corresp. 1]

[1] College of Forestry, Key Laboratory of State Forestry Administration for Silviculture of the Lower Yellow River, Shandong Agricultural University, Tai'an, Shandong province, China

[2] Laboratory of Systematic Evolution and Biogeography of Woody Plants, School of Ecology and Nature Conservation, Beijing Forestry University, Beijing, China

[3] Forestry Bureau of Huguan County, Changzhi, Shanxi Province, China

[4] Forestry Conservation and Development Center of Ningyang County, Ningyang, Tai'an, Shandong Province, China

Corresponding Author: Zhen Feng
Email address: fengzn408@qq.com

Background. Polyploidy plays an important role in plant breeding and has widespread effects on photosynthetic capacity. To determine the photosynthetic capacity of the tetraploid variety *Acer buergerianum* Miq. 'Xingwang', we compared the gas exchange parameters, chloroplast structure, chlorophyll contents, and chlorophyll fluorescence parameters between the tetraploid *Acer buergerianum* 'Xingwang' and the diploid 'S4'. To evaluate the effects of genome duplication on the photosynthetic capacity of *Acer buergerianum* 'Xingwang', the transcriptomes of the autotetraploid 'Xingwang' and the diploid 'S4' of *A. buergerianum* were compared. **Methods.** The ploidy of *Acer buergerianum* 'Xingwang' was identified by flow cytometry and the chromosome counting method. An LI-6800 portable photosynthesis system analyzer was used to assess the gas exchange parameters of the tetraploid variety 'Xingwang' and diploid variety 'S4' of *A. buergerianum*. We used a BioMate 3S ultraviolet-visible spectrophotometer and portable modulated fluorometer to measure the chlorophyll contents and chlorophyll fluorescence parameters, respectively, of 'Xingwang' and 'S4'. Illumina high-throughput sequencing technology was used to identify the differences in the genes involved in the photosynthetic differences and determine their expression characteristics. **Results.** The single-cell DNA content and chromosome number of the tetraploid 'Xingwang' were twice those found in the normal diploid 'S4'. In terms of gas exchange parameters, the change in stomatal conductance, change in intercellular CO_2 concentration, transpiration rate and net photosynthetic rate of 'Xingwang' were higher than those of the diploid 'S4'. The chlorophyll contents, the maximal photochemical efficiency of PSII and the potential photochemical efficiency of PSII in 'Xingwang' were higher than those of 'S4'. The chloroplasts of 'Xingwang' contained thicker thylakoid lamellae. By the use of Illumina

sequencing technology, a total of 51807 unigenes were obtained; they had an average length of 1487 nt, and the average N50 was 2034 nt. The lengths of most of the unigenes obtained ranged from 200-300 bp, with an average value of 5262, followed by those longer than 3000 bp, with an average value of 4791. The data revealed numerous differences in gene expression between the two transcriptomes. In total, 24221 differentially expressed genes were screened, and the percentage of differentially expressed genes was as high as 46.75% (24224/51807), of which 10474 genes were upregulated and 13747 genes were downregulated. We analyzed the key genes in the photosynthesis pathway and the porphyrin and chlorophyll metabolism pathway; the upregulation of HemB may promote an increase in the chlorophyll contents of 'Xingwang', and the upregulation of related genes in PSII and PSI may enhance the light harvesting of 'Xingwang', increasing its light energy conversion efficiency.

Ploidy level enhances the photosynthetic capacity of a tetraploid variety of *Acer buergerianum* Miq.

6   Yi Wang[1, 2]   Bingyu Jia[1, 3]   Hongjian Ren[4]   Zhen Feng[1]

8   [1] College of Forestry, Shandong Agricultural University, Key Laboratory of State Forestry
9   Administration for Silviculture of the Lower Yellow River, Shandong, China
10 [2] Laboratory of Systematic Evolution and Biogeography of Woody Plants, School of Ecology
11 and Nature Conservation, Beijing Forestry University
12 [3] Forestry Bureau of Huguan County, Changzhi, Shanxi, China
13 [4] Forestry Conservation and Development Center of Ningyang County, Tai'an, Shandong, China

15 Yi Wang and Bingyu Jia contributed equally to this work.

16 Corresponding Author:

17 Zhen Feng[1]

18 No. 61 Daizong Street, Shandong Agricultural University, Tai'an, Shandong, 271000, China

19 Email address: fengzn408@qq.com

Abstract

22 **Background.** Polyploidy plays an important role in plant breeding and has widespread effects on

23 photosynthetic capacity. To determine the photosynthetic capacity of the tetraploid variety *Acer*

24 *buergerianum* Miq. 'Xingwang', we compared the gas exchange parameters, chloroplast structure,

25 chlorophyll contents, and chlorophyll fluorescence parameters between the tetraploid *Acer*

26 *buergerianum* 'Xingwang' and the diploid 'S4'. To evaluate the effects of genome duplication on

27 the photosynthetic capacity of *Acer buergerianum* 'Xingwang', the transcriptomes of the

28   autotetraploid 'Xingwang' and the diploid 'S4' of *A. buergerianum* were compared.

29   **Methods.** The ploidy of *Acer buergerianum* 'Xingwang' was identified by flow cytometry and

30   the chromosome counting method. An LI-6800 portable photosynthesis system analyzer was

31   used to assess the gas exchange parameters of the tetraploid variety 'Xingwang' and diploid

32   variety 'S4' of *Acer buergerianum*. We used a BioMate 3S ultraviolet-visible spectrophotometer

33   and portable modulated fluorometer to measure the chlorophyll contents and chlorophyll

34   fluorescence parameters, respectively, of 'Xingwang' and 'S4'. Illumina high-throughput

35   sequencing technology was used to identify the differences in the genes involved in the

36   photosynthetic differences and determine their expression characteristics.

37   **Results.** The single-cell DNA content and chromosome number of the tetraploid 'Xingwang'

38   were twice those found in the normal diploid 'S4'. In terms of gas exchange parameters, the

39   change in stomatal conductance, change in intercellular CO_2 concentration, transpiration rate and

40   net photosynthetic rate of 'Xingwang' were higher than those of the diploid 'S4'. The chlorophyll

41   contents, the maximal photochemical efficiency of PSII and the potential photochemical

42   efficiency of PSII in 'Xingwang' were higher than those of 'S4'. The chloroplasts of 'Xingwang'

43   contained thicker thylakoid lamellae. By the use of Illumina sequencing technology, a total of

44   51797 unigenes were obtained; they had an average length of 1487 nt, and the average N50 was

45   2034 nt. The lengths of most of the unigenes obtained ranged from 200-300 bp, with a number of

46   5258, followed by those longer than 3000 bp, with a number of 4791. The data revealed

47   numerous differences in gene expression between the two transcriptomes. In total, 24221

48   differentially expressed genes were screened, and the percentage of differentially expressed

49   genes was as high as 46.76% (24221/51797), of which 10474 genes were upregulated and 13747

50   genes were downregulated. We analyzed the key genes in the photosynthesis pathway and the

51   porphyrin and chlorophyll metabolism pathway; the upregulation of HemB may promote an

52   increase in the chlorophyll contents of 'Xingwang', and the upregulation of related genes in PSII

53   and PSI may enhance the light harvesting of 'Xingwang', increasing its light energy conversion

54   efficiency.

55

Introduction

57

58   Polyploidy plays an important role in plant breeding (Otto, 2007; Dhooghe et al., 2011)

59   because polyploid plants often more strongly express the characteristics targeted by breeders—

60   including traits related to morphology, metabolism, genetic adaptation ability and tolerance—

61   than their diploid counterparts (Comai, 2005; Leal- Bertioli, 2017). Polyploid plant growth may

62   require more energy and carbohydrates (Evans, 2013), which are primarily obtained from the

63   process of photosynthetic carbon assimilation in the leaves; therefore, the enhanced

64   photosynthetic capacity of polyploids compared to diploids may be advantageous (Evans, 2013).

65   Photosynthetic capacity is related to the chlorophyll content, the structure of chloroplasts, and

66   related gene expression resulting from the polyploidization event. In terms of chlorophyll

67   contents and the structure of chloroplasts, chloroplasts contain chlorophyll, which is the site of

68   photosynthesis, so the effect of chlorophyll contents and the structure of chloroplasts on

69   photosynthetic capacity is very obvious (Eckhardt, Grimm & Hörtensteiner, 2004). Previous

70   reports showed that tetraploids of *C. nankingense* had significantly higher chlorophyll a and b

71   contents than diploids and increased photosynthetic capacity (Dong et al., 2017). In an

72   ultrastructural study of polyploid chloroplasts and their characteristics at the transcriptome level,

73   Chen et al. (2010) found that the number of chloroplasts, grana and lamellae in heterotetraploids

74   of *Cucumis* was higher than that in diploids. Zhu et al. (2012) also found that the chloroplasts,

75   grana and lamellae in tetraploids were present in greater numbers than in diploids during their

76   comparison of the leaf ultrastructure of watermelon seedlings with different ploidy. In previous

77   studies on the ultrastructure of chloroplasts, changes in the plastoglobuli in chloroplasts were

78   ignored. The so-called plastoglobuli are also called plastid globules and lipidosomes because of

79   their storage of fat (Wang, 2000). The plastoglobule in the chromoplast may be the product of

80   the disintegration of the thylakoid membrane. With the disintegration of thylakoids, the number

81   of plastoglobuli increases, and therefore, this number may be related to whether the thylakoid

82   membrane structure is stable (Greenwood et al., 1963). The thylakoid membrane contains

83   photosynthetic pigments and a variety of protein molecules and undergoes reactions such as

84   those involving light energy absorption, transfer and transformation, and electron transfer;

85   therefore, the number and structure of thylakoids are important factors that influence

86   photosynthesis (Allen & Forsberg, 2001; Liu, 2012). Dong et al. (2017) found that whole

87   genome duplication enhances the photosynthetic capacity of *C. nankingense*, mainly because the

88   number of genes associated with chlorophyll synthesis was upregulated in the tetraploid form,

89   while those associated with chlorophyll degradation were downregulated.

90   The photosynthetic rate of plant cells is related to the DNA content of the cell itself; thus,

91   the increased DNA content in polyploid mesophyll cells may endow them with a higher

92   photosynthetic rate (Coate et al., 2012; Warner and Edwards, 1993). However, for different

93   plants, the number of mesophyll cells per unit area changes with the increase in cell volume

94   (Warner and Edwards, 1993); thus, at the leaf level, the effect of polyploidy on the

95   photosynthetic capacity will vary from species to species. Therefore, in some plants, the

96   photosynthetic rate of tetraploids is higher than that of diploids, such as *Paulownia australis*.

97   (Wang et al., 2013). Studies have also shown that the photosynthetic rate of some tetraploids is

98   lower than that of their diploid counterparts, as is the case for *Fragaria* (Gao et al., 2017).

99   *Acer buergerianum* belongs to the Sapindaceae family, and it is native to eastern China

100   (Hayashi, 2007) and Japan (Matsue & Takeda, 2009). In China, *Acer buergerianum* is mainly

101   distributed across the middle and lower reaches of the Yangtze River and the Taiwan region

102   (Chinese Flora Editorial Board of the Chinese Academy of Sciences, 1981). *Acer buergerianum*

103   is highly adaptable, drought-resistant, and has excellent wood. It is also an important color-leaf

104   tree species and forest landscape resource (Feng et al., 2012; Guo et al., 2013). Therefore,

105   vigorously developing *Acer buergerianum* is of great interest for improving the ecological

106   environment and improving people's living standards. However, research on *Acer buergerianum*

107   is mainly focused on landscape applications, and there is less research on its polyploid

108   photosynthetic capacity and chloroplast ultrastructure and on the transcriptomic analysis of

109   photosynthesis in this species, which limits its development. The chromosome cardinality of *A.*

110   *buergerianum* is 13, the number of diploid chromosomes is 2n = 2x = 26 (Xu, 1998), and the

111   number of tetraploid chromosomes is 2n = 4x = 52 (Xu, 1998). *Acer buergerianum* 'Xingwang'

112   is a tetraploid and is propagated by grafting. In our previous research, the tetraploid 'Xingwang'

113   showed a significant advantage over diploid plants in terms of vegetative growth, including leaf

114   length, leaf width, and leaf thickness (An et al., 2018). Since the increased carbohydrate

115   accumulation required for enhanced vegetative growth is closely associated with more effective

116   photosynthesis (Warner and Edwards, 1993), vegetative growth superiority might indicate

117   improved photosynthetic performance in the tetraploid *Acer buergerianum*.

118   To reveal the photosynthetic capacity of the tetraploid *Acer buergerianum* 'Xingwang', we

119   compared the differences between the gas exchange parameters, chlorophyll contents,

120   chlorophyll fluorescence parameters and chloroplast ultrastructure of the diploid 'S4' and the

121   autotetraploid 'Xingwang'. Additionally, comparisons between the transcriptomes of the

122   autotetraploid 'Xingwang' and its diploid relative regarding photosynthesis were performed

123   using Illumina high-throughput sequencing technology. This study lays a foundation for an in-

124   depth understanding of the tetraploid variety *A. buergerianum* 'Xingwang' and the genetic

125   engineering of this species.

126

127

128

Materials & Methods

129

130

Plant materials

131

132

133   The autotetraploid 'Xingwang' (X) originated from the colchicine-induced somatic chromosome

134   doubling of the diploid 'S4' (S), and twenty clones with genetic consistency were obtained by

135   grafting propagation. Young leaves of six-year-old 'Xingwang' and autodiploid 'S4' were used as

136   experimental materials. All the test materials were obtained from the gardens of Shandong

137   Agricultural University Forestry College (N36°10' 12.44'', E117°09' 40.33'') and were grown

138   outdoors. The region has a temperate monsoon climate with an average annual temperature of

139   13°C, average annual precipitation of 688.3 mm, and annual average relative humidity of 66%.

140   The soil is loamy.

141

142   **Polyploidy identification**

143

144   The single-cell DNA content of the polyploid X was determined by flow cytometry (Handyem

145   HPC-150, Canada) (Zhang, Guo & Deng, 2006). Normal leaves of X and S were collected; the

146   leaves were washed, and the veins were removed. Then, 20 mg of the remaining leaf tissue was

147   placed in a culture dish, and fresh lysis solution was added. A double-sided blade was used to

148   chop the leaf tissue quickly in a Petri dish, and the tissue was processed for 3-5 min. A pipette

149   was used to extract 1 ml of the chopped sample, which was filtered into a 1.5 ml centrifuge tube

150   with a 300-mesh nylon sieve. Then, 1 mg/ml propidium iodide solution was added to the

151   centrifuge tube to reach a final propidium iodide concentration of 0.1 mg/ml, and the solution

152   was allowed to stand for 5 min. The processed solution was filtered through a 300-mesh nylon

153   sieve again into a new centrifuge tube and then tested on the machine. Three replicates were

154   employed for each test sample from the same plant, and at least 9000 cells were collected each

155   time. The lysate formulation was 0.1 mol/l citric acid, 0.5% TWEEN-20, 0.4 mol/l disodium

156   hydrogen phosphate, and 1% PVP-10 (Kron & Husband, 2012).

157   Chromosome ploidy identification of the polyploid X was performed using the chromosome

158   counting method (Zhang et al., 2005). The innermost 0.5 cm length of the stem tip was selected

159   as the experimental material, which was treated at -20°C for 18 h in a stable solution (anhydrous

160   ethanol:glacial acetic acid:trichloromethane = 5:3:2) and then stored in 75% alcohol at 4°C. The

161   material was removed and washed 3 times in ultrapure water. The excess water was absorbed

162   with clean filter paper and the sample was transferred to 0.075 mol/l KCl solution to reach

163   hypotonicity for 30 min. Following dissociation, the material was rinsed with ultrapure water 3

164   times and placed in ultrapure water for 30 min to become hypotonic. The water and Carbo

165   Fuchsin dye (Solarbio, China) solution were then absorbed for 15-20 min, the material was

166   pressed into a tablet, and 10-20 relatively clear metaphase cells were found under the microscope

167   for identification.

168

169   **Gas exchange parameters**

170

171   The experimental site is in the garden of Shandong Agricultural University Forestry College (the

172   environmental conditions are the same as those detailed above). We chose a sunny day in the

173   middle of each month from May to September 2019 and selected tetraploid X and diploid S

174   plants of equal size. We used an LI-6800 portable photosynthesis system (LI-COR, USA) to

175   measure the net photosynthetic rate (P_n), stomatal conductance (G_s), transpiration rate (T_r), and

176   intercellular carbon dioxide concentration (C_i) of the third pair of sun-exposed, physiologically

177   mature leaves from the top of the side branch to the trunk at the same orientation from 3 plants,

178   with 3 leaves collected from each plant. The gas exchange parameter data were recorded every

179   two hours from 8:00 to 18:00, and the average value was used for the processing analysis.

180

181   **Determination of chlorophyll contents and chlorophyll fluorescence parameters**

182

183   Fresh leaves from diploid and tetraploid plants were cut into pieces and submerged in 80% (v/v)

184   acetone in the dark at room temperature to extract their chlorophyll (Arnon, 1949). The

185   chlorophyll a (Chl a), chlorophyll b (Chl b) and total chlorophyll (a+b) contents were measured

186   using a BioMate 3S ultraviolet-visible spectrophotometer (Thermo Fisher Scientific Inc., USA)

187   at 470, 649, and 665 nm according to the methods of Li (2000).

188   The chloroplast fluorescence parameters of the X and S leaves were measured under slightly

189   excessive light stress. The control group was exposed to a natural light intensity (88000 lx) while

190   the experimental group was exposed to a 20% increased light intensity (105600 lx). The

191   chlorophyll fluorescence parameters were measured using a portable modulated fluorometer

192   (PAM-2500, Heinz Walz, Germany). The maximal fluorescence (F_m) and the minimal

193   fluorescence (F_o) were recorded. The maximal photochemical efficiency of PSII (F_v/F_m) and the

194   potential photochemical efficiency of PSII (F_v/F_o) were calculated as $F_v/F_m = (F_m - F_o)/F_m$ and

195    $F_v/F_o = (F_m - F_o)/F_o$ (Kramer et al., 2004).

196   Nine samples from three individuals of each ploidy type were measured.

197

198   **Electron microscope sample preparation of leaf chloroplasts**

199

200   The mature leaves on the annual sun-exposed branches were collected at 4°C, and the container

201   and instruments were precooled. Fresh leaf samples (1 mm×1 mm) were cut from the middle part

202   of the leaves along the main vein, fixed in 2.5% glutaraldehyde fixative solution, and stored at

203   4°C. The fixed leaves were washed 3 times with 0.1 mol/l phosphate buffer solution containing 1%

204   osmium acid (Pelco, EM level, USA) at 4°C for 3 h, washed 3 times with buffer solution, and

205   then dehydrated step by step with ethanol and propylene oxide. A replacement was performed;

206   then, the embedding material was impregnated with Spurr resin (Spi-Chem, USA). Last, the

207   samples were polymerized in an oven at 70°C. The embedding blocks of the different materials

208   were placed on an ultrathin microtome (Leica EM UC6, Germany) for sectioning. The thickness

209   of the ultrathin sections was 70 nm. The sections were stained with uranyl acetate (Spi-Chem,

210   ACS level, USA) and lead citrate trihydrate (Spi-Chem, ACS level, USA) and observed and

211   photographed under a transmission electron microscope (JEM1230, JEOL, Japan). Image-Pro

212   Plus 6.0 (Media Cybernetics, Inc. USA) was used to produce statistics on the thylakoid lamella

213   thickness. Three samples of X and S were analyzed, and for each sample, the thylakoid lamella

214   thickness and number of plastoglobules from at least three chloroplasts were detected.

215

216   **RNA extraction, library construction and RNA-seq**

217

218 During the transcriptome sequencing process, for X and S, three biological replicates were taken

219 from the same plant, and they were denoted X1, X2, and X3 and S1, S2, and S3. Tender leaves

220 from the annual sunny branches were obtained, and an Adelaide Biologicals EASYspin Plant

221 RNA Quick Extraction Kit was used to extract the total RNA from each X and S sample. A

222 spectrophotometer (Thermo Fisher Scientific, Inc., USA) was used for RNA quality inspection,

223 and the integrity of the RNA was confirmed by 1% agarose gel electrophoresis.

224   Oligo (dT) magnetic beads were used to enrich the mRNA with a polyA tail, and

225 interrupting buffer was used to fragment the resulting RNA. Random N6 primers were used for

226 reverse transcription, and two strands of cDNA were synthesized to form double-stranded DNA.

227 The ends of synthetic double-stranded DNA were filled in, and the 5' end was phosphorylated.

228 The 3' end forms a sticky end that protrudes with a base 'A'; then, there is a complementary end

229 with a protruding base 'T' on the 5' end, and the ligated product was amplified by PCR with

230 specific primers. The PCR products were thermally denatured into single-stranded DNA, and

231 then the single-stranded DNA was circularized with a bridge primer to obtain a single-stranded

232 circular DNA library. Finally, the BGISEQ-500 platform was used to obtain raw sequencing data.

233

234 ***De novo* assembly and functional annotation**

235

236 The software SOAPnuke (Cock et al., 2010) was used to filter the raw data for sequencing, and

237 the filtered data were called clean reads and saved in FASTQ format. Trinity software (Grabherr

238 et al., 2011) was used to assemble then process clean reads in turn. Trinity has three independent

239 modules: Inchworm, Chrysalis and Butterfly. The data were first assembled with Inchworm to

240 obtain the full-length isoform transcript data and the fragment form of the isoform-containing

241 transcript. Next, in the Chrysalis module, the contigs that may have variable splicing and parallel

242 genes are clustered to construct a large number of individual de Bruijn maps. Last, the linear path

243 is merged with continuous nodes in the de Bruijn maps in the Butterfly module and full-length

244 transcript splicing subtypes are extracted.

245 Then, TGICL software (Pertea et al., 2003) was used to cluster the transcripts to remove

246 redundancies and obtain the unigenes. After clustering, the unigenes were divided into two

247 classes: clusters with the prefix CL and singletons with the prefix Unigene.

248   For the resulting transcript data, we used Trinity to perform open reading frame (ORF)

249 predictions, and we annotated the transcript with complete ORFs. After assembling the unigenes,

250 we performed bioinformatics analysis and aligned the predicted protein sequences to six

251 functional databases, namely, NCBI nonredundant protein (Nr), NCBI nucleotide in sequences

252 (NT), Swiss-Prot, Pfam, Kyoto Encyclopedia of Genes and Genomes (KEGG), euKaryotic

253 Orthologous Groups (KOG), and Gene Ontology (GO), for annotation and classification. The

254 best alignment results were used to annotate the transcriptome sequences and to determine the

255 orientation of the sequences. The All-unigene results aligmented to the NR database were

256 annotated to the GO database via Blast2GO software (Conesa et al., 2005), and the metabolic

257 pathways were compared with the KEGG database (Kanehisa et al., 2008).

258

259 **Differential gene analysis**

260

261   The DEGseq method (Wang et al., 2010) was used to detect differentially expressed genes

262 (DEGs), calculate the P-values (P-value, hypothesis test probability) and correct the P-values to

263 Q-values. To improve the accuracy of the DEGs, we implemented the fold change as more than

264 twice (fold change $\geq$ 2.00) and the Q-values (adjusted P-value) $\leq$ 0.05 to screen differential

265 genes and detect the DEGs based on the principle of a negative binomial distribution. The DEGs

266 related to photosynthetic characteristics were selected for analysis.

267

268 **Real-time quantitative RT-PCR (qRT-PCR) verification**

269

270 To confirm the reliability of the sequencing analysis, the expression of the candidate genes was

271 measured by qRT-PCR. First, ABM's 5X All-In-One RT MasterMix Kit (with the AccuRT

272 Genomic DNA Removal Kit) was used to reverse transcribe the RNA into the first strand of

273 cDNA, and the product was stored at -20°C. Nine candidate genes were selected, the sequences

274 of the target genes were obtained from the transcriptome results (Table S1), and primers were

275 designed. TUB was used as the internal reference gene, and a Bio-Rad CFX96TM Real-Time

276 PCR instrument was used to complete the qRT-PCR. The reaction procedure was as follows:

277 95°C for 30 s; 39 cycles of 95°C for 5 s and 60°C for 30 s; and then 95°C for 10 s. The qRT-

278 PCR results were calculated using the $2^{-\triangle\triangle t}$ method, and whether the expression trend of the

279 transcriptome results was consistent with the verification results was assessed. The sequences of

280 the primers used are shown in Table S2.

281

Statistical analysis

283

284 Descriptive statistical analyses were used for the measured parameters to obtain the means and

285 standard errors (SEs). One-way analysis of variance (ANOVA) was used to analyze the

286 significance of the differences in the gas exchange parameters, chlorophyll contents, chlorophyll

287 fluorescence parameters and chloroplast ultrastructure between X and S, with the ploidy level as

288 a fixed factor. The significance level was set at $p < 0.05$. Statistical analyses were performed

289 with SPSS 16.0 (SPSS, Inc., Chicago, IL, USA).

290

Results

292

Identification of the *A. buergerianum* tetraploid

294

295 By observing the stem tip under the microscope, we found that the chromosome number of X

296 was significantly higher than that of S by twofold (Fig. S1).

297 The DNA content in a single cell was detected by flow cytometry, and the results are shown in

298 Fig. S2. The ploidy level of the plant can be inferred from the peak figure of its relative DNA

299 content (Dole el, Greilhuber & Suda, 2007; Paul & Husband, 2012). The main peak single-cell

300 DNA content in the S leaves was at channel 100, while the main peak single-cell DNA content in

301 X leaves was at channel 200. Thus, the single-cell DNA content of X was twice that of S;

302 therefore, X was determined to be tetraploid.

303

304 **Gas exchange parameters, chlorophyll contents and chlorophyll fluorescence**

305 **parameters**

306

307 Similar patterns of diurnal changes in T_r were observed between diploid and tetraploid $A.$

308 *buergerianum* X and S leaves from May to September (Fig. S3). In May, July, and September, a

309 single-peak curve was observed that first increased and then decreased, reaching a maximum at

310 approximately 12:00. The peak T_r of X was higher than that of S, the T_r reached the maximum in

311 July, the maximum T_r of X was 1.33 mol·m^{-2}·s^{-1}, and the maximum T_r of S was 1.23 mol·m^{-2}·s^{-1}.

312 In June and August, the daily variation of the whole day showed a double-peak curve, with the

313 first peak appearing at approximately 10:00 and the second peak appearing at 14:00. In X and S,

314 the first peak was greater than the second peak and fell into a valley at approximately 12:00.

315 The daily variation trends in the P_n of X and S leaves from May to September were similar

316 (Fig. S4). In May, July, and September, a single-peak curve first increased and then decreased.

317 Starting at 8:00, the Pn gradually increased, reached a maximum at approximately 12:00, and

318 then gradually decreased; the P_n reached its maximum in August. The peak P_n of X was higher

319 than that of S. The maximum P_n of X was 11.15 μmol·m^{-2}·s^{-1}, and the average P_n was 6.63

320 μmol·m^{-2}·s^{-1}. The maximum P_n of S was 8.56 μmol·m^{-2}·s^{-1}, and the average P_n was 5.72

321 μmol·m^{-2}·s^{-1}. The diurnal changes in June and August showed a double-peaked curve. The first

322 peak appeared at approximately 10:00, and the second peak appeared at 14:00. The first peaks of

323 X and S were both higher than the second peak, and the values fell into a valley at approximately

324 12:00. Over the five months from May to September, the maximum P_n of X increased by 4.31%,

325   12.35%, 8.48%, 30.31%, and 7.76% over S.

326   The diurnal variation in G_s of X and S leaves from May to September was similar, and the G_s

327   of X during different months was higher than that of S (Fig. S5). X and S showed a single-peak

328   curve that first increased and then decreased in May, July, and September and was lower at 8:00

329   and 18:00. Starting from 8:00, G_s gradually increased and reached a maximum at approximately

330   12:00. The diurnal changes in June and August showed a bimodal curve. The peak G_s of X was

331   higher than that of S, and the G_s of X and S reached their maximum levels in August. In June,

332   the first peaks of X and S both appeared at approximately 10:00, and the second peak appeared at

333   14:00. The first peaks of X and S both appeared at approximately 10:00 in August, and the

334   second peaks appeared at approximately 14:00 for X and at approximately 16:00 for S. The first

335   peaks of X and S were both larger than the second peaks, and their values fell into a valley at

336   approximately 12:00.

337   From May to September, the daily change curve in C_i between X and S cells presented a

338   single valley change (Fig. S6). The diurnal variation curves of X and S both first decreased   and

339   then increased, and the C_i of X was greater than that of S during different months. Starting from

340   8:00, as the environmental conditions changed, the C_i gradually decreased, and the lowest value

341   appeared at approximately 12:00 and then gradually increased.

342   Among the gas exchange parameters of tetraploid X and diploid S, T_r, P_n, G_s and C_i all

343   exhibited extremely significant differences (P < 0.01). From May to September, the maximum

344   values of all the gas exchange parameters of X were higher than those of S (Table 1).

345   The analysis of chlorophyll contents showed that the Chl a, Chl b and total chlorophyll

346   contents were significantly higher in X than in S (Fig. 1A). The total chlorophyll contents of X

347   and S were 2.47 mg·g^{-1} and 1.52 mg·g^{-1}, respectively. The leaves of X contained 38.66% more

348   chlorophyll than those of S. Under slightly excessive light stress, F_v/F_m was 0.77 and 0.83 and

349   F_v/F_o was 3.45 and 4.95 in S and X, respectively, and these values were significantly different

350   (Fig. 1B).

351

352   **Ultrastructure of the chloroplast**

353

354   The ultrastructures of X and S mesophyll cell chloroplasts were further compared using a

355   transmission electron microscope (Fig. 2). The chloroplasts of X and S were well developed,

356   with obvious thylakoids and stacked basal particles. However, differences were observed in the

357   internal structure of the chloroplasts from the two varieties. Compared with the chloroplasts in S,

358   the chloroplasts in X contained thylakoid lamellae that were twice as thick (Fig. 2, Fig. 3A). In

359   addition, the thylakoid lamellae of X were arranged more closely than those of S, and more

360   starch grains were observed in S. In the chloroplasts of the tetraploid X, the number of

361   plastoglobules was lower than that of the diploid S (Fig. 3B).

362

363   **Transcriptome sequencing and assembly**

364

365   The transcriptomes of X and S produced 42,804,595 nt and 44,971,637 nt raw data, respectively,

366   and the Q20 percentages were both over 97%.

367   The unigenes in each sample were clustered to eliminate redundancy, and 51797 unigenes

368   were obtained, with an average length of 1487 nt; the average N50 was 2034 nt.

369

370   **Transcript database annotation**

371

372   A total of 44665 unigenes were annotated and accounted for 86.23% of all the unigenes. The

373   numbers of unigenes annotated in the NR, NT, SwissProt, KEGG, KOG, Pfam, and GO

374   functional databases were 43076, 36463, 32865, 34715, 34085, 34599, and 26781, respectively

375   (Table S3), (Fig. S7).

376

377   **Analysis of DEGs**

378

379   A total of 24221 DEGs (Table S4) were screened between the *Acer buergerianum* diploid and

380   tetraploid transcriptomes, and they included 10474 upregulated genes and 13747 downregulated

381   genes. To study the function of DEGs related to photosynthetic characteristics in diploid and

382   tetraploid plants, GO (Table S5) and KEGG (Table S6) classifications were determined.

383   We analyzed the pathways of porphyrin and chlorophyll metabolism and photosynthesis.

384   During chlorophyll synthesis in *A. buergerianum*, 5 genes encoding HemB were identified, all of

385   which were upregulated. One gene encoded HemC, and its expression was downregulated. One

386   gene encoded HemE, and its expression was downregulated. Three genes encoded CHLH/D/I; 1

387   was upregulated, while 2 were downregulated (Fig. S8, Table 2) (Matsumoto et al, 2004; Beale,

388   2005).

389   In this study, 58 DEGs were annotated as being related to the photosynthesis pathway, with

390   30 upregulated genes and 28 downregulated genes. Twelve were photosystem I (PSI)-related

391   genes, of which the PsaA-, PsaB-, and PsaK-related genes were upregulated and the PsaG- and

392   PsaH-related genes were downregulated; 28 were photosystem II (PSII)-related genes, of which

393   the PsbE- and Psb27-related genes were upregulated and the PsbH-, PsbQ-, and PsbS-related

394   genes were downregulated; 4 were cytochrome b6/f complex-related genes, of which the PetB-

395   and PetC-related genes were downregulated; 10 were photosynthetic electron transport-related

396   genes, of which the PetH-related genes were downregulated; 8 were F-type ATPase-related

397   genes, among which the beta-, delta-, and b-related genes were upregulated (Fig. 4) (Yamori &

398   Shikanai, 2016).

399

400   **qRT-PCR validation of the candidate DEGs**

401

402   To verify the reliability of the transcriptome sequencing results, qRT-PCR validation was

403   performed on 9 randomly selected candidate genes (Table S1), including four upregulated genes

404   (CL6641.Contig2_All, CL2285.Contig2_All, CL3396.Contig3_All, and CL335.Contig5_All)

405   and five downregulated genes (CL7423.Contig2_All, Unigene5873_All, CL1401.Contig2_All,

406   CL6251.Contig1_All, and CL5835.Contig1_All). The results were consistent with the expression

407   patterns of the transcriptome sequencing results (Fig. S9), validating the transcriptome

408   sequencing results obtained in this study.

409

410   **Discussion**

411

412   A comparison of the gas exchange parameters for X and S showed that X plants had a higher

413   P_n, T_r, G_s, and C_i than S plants, which indicates that the gas exchange parameters of the

414   tetraploid form of X were markedly higher those that of the diploid form of S. The P_n of X and S

415   their maximum levels in August, which may be due to favorable conditions for the growth of *A.*

416   *buergerianum* such as the photoperiod and light intensity, temperature, and relative humidity

417   (Wang et al., 2006). Among the gas exchange parameters for X and S photosynthesis, the daily

418   variation curves in the P_n and G_s show different changes during different months. The G_s and C_i

419   of tetraploid X were higher than those of S, so the P_n differences between X and S may come

420   from stomatal factors. The increase in the stomatal conductance of X is conducive to the

421   continuous replenishment of CO_2 in the intercellular space during photosynthesis, thus

422   maintaining a high intercellular CO_2 concentration and lower stomatal limitation (Du et al.,

423   2011); as a result, the P_n of X was significantly higher than that of S. This result was consistent

424   with a previous study showing that stomata from X were significantly larger than those from S

425   (An et al., 2018).

426   Chloroplasts are the main location for photosynthesis in plants, and their structure directly

427   affects the photosynthesis and characteristics of leaves (Liu, 2012). Chen et al. (2010) used

428   diploid melon, allogeneic triploid and allogeneic tetraploid plants as test materials to compare the

429   differences in chloroplast ultrastructure, and the results showed that the number of chloroplasts,

430   basal grains and lamellae increased significantly in the allotetraploids compared to the diploids.

431   However, many previous studies have ignored the changes in thylakoids. In this study, there

432   were more and thicker thylakoid lamellae in X than in S, and the arrangement of thylakoids was

433   more densely stacked in the basal granule, which indicated that their daylighting mechanism was

434   more effective at absorbing and converting light energy (Li, 2018). In addition, the number of

435   plastoglobules in X was lower than that in S, which may indicate that the thylakoid membrane

436   structure of X was relatively stable. These differences may be one of the factors that cause the

437   photosynthetic rate of the tetraploid X to be higher than that of the diploid S.

438   Chlorophyll is the key photosynthetic pigment in higher plants (Masuda and Fujita, 2008).

439   When plants are deficient in chlorophyll, abnormal thylakoid structure development often occurs

440   (Falbel & Staehelin, 2008). The synthesis and degradation of chlorophyll affect the development

441   of chloroplasts and further affect the photosynthesis of plants (Eckhardt, Grimm & Hörtensteiner,

442   2004). Here, the chlorophyll content of X was significantly increased compared with that of S,

443   which was also an important factor that made the photosynthetic capacity of X significantly

444   stronger than that of S.

445   The increase in chlorophyll content in X was presumably associated with the upregulation of

446   the chlorophyll synthesis genes HemB caused by whole genome duplication. Green plants need

447   to complete 16 steps to synthesize chlorophyll; the synthesis of chlorophyll b involves four

448   processes, 5-aminolevulinic acid (ALA) synthesis, protoporphyrin synthesis, the conversion of

449   protoporphyrin to protochlorophyll, and the conversion of protochlorophyll to chlorophyll a and

450   b (Fig. S8) (Ohmiya et al., 2014). Here, among the genes involved in chlorophyll synthesis,

451   HemB in X underwent major changes, and all five genes involved in HemB were upregulated.

452   The expression of HemB (which encodes aminolevulinate dehydratase, ALAD) has a positive

453   regulatory effect on chlorophyll biosynthesis (Tang et al., 2012); therefore, the upregulation of

454   the gene encoding HemB may result in increased chlorophyll synthesis, thereby promoting the

455   photosynthesis of tetraploids. This finding is consistent with the significantly higher chlorophyll

456   contents in X than in S.

457   Research has shown that the genes encoding the components of PS II and PS I are associated

458   with dosage sensitivity (Coate et al., 2014). In many cases, gene dose sensitivity correlates with

459   gene duplication, as described by the gene balance theory (Edger & Pires, 2009). During

460   photosynthesis, *psaA* and *psaB* are mainly related to light harvesting (Chitnis, 1996); thus, the

461   upregulation of their related genes may enhance the light harvesting of X. In addition, the

462   differential expression of the related genes in PS II may promote the efficiency of solar energy

463   conversion into chemical energy. This hypothesis was confirmed by measurements of the X and

464   S fluorescence parameters. Under mild light stress, the F_v/F_o and F_v/F_m of X were significantly

465   higher than those of S, indicating that the autotetraploid had higher light harvesting and

466   conversion efficiency than its diploid (Liang et al., 2004). The chloroplast ATPase on the

467   thylakoid membrane is responsible for catalyzing light-driven ATP synthesis and providing

468   energy for carbon fixation in photosynthesis (Zhang et al., 2018); therefore, the upregulation of

469   related genes in ATPase may provide more energy for carbon fixation in photosynthesis, thereby

470   increasing the photosynthetic efficiency of polyploid X and meeting its growth needs. Finally,

471   we present a schematic diagram for the possible mechanisms to show the reasons for the

472   increased photosynthetic capacity of X (Fig. 5).

473

Conclusions

475

476   In this study, ploidy identification of the variety *Acer buergerianum* 'Xingwang' confirmed that it

477   is a tetraploid. The gas exchange parameters, chlorophyll contents, F_v/F_o and F_v/F_m of the

478   tetraploid 'Xingwang' were significantly higher than those of the diploid 'S4'. Moreover,

479   'Xingwang' has a thicker thylakoid lamella and fewer plastoglobules than 'S4'. These reasons

480   cause 'Xingwang' to have a higher photosynthetic capacity than 'S4'. The transcriptomes of the

481   autotetraploid 'Xingwang' and diploid 'S4' were compared. We analyzed the key genes of the

482   photosynthesis pathway and the porphyrin and chlorophyll metabolism pathway, and the

483   upregulation of HemB may promote the increased chlorophyll contents of 'Xingwang'. The

484   upregulation of the related genes whose products encode components of PSII and PSI may

485   enhance the light harvesting of 'Xingwang', increasing its light energy conversion efficiency.

486

487

Acknowledgments

489

490   We thank Fenfen Si of Shandong Agricultural University for assistance with the experimental

491   methods.

492

References

494

495 **An K, Feng Z, Qiao Q, Ren HJ. 2018.** Identification of Natural Tetraploid Variant in *Acer.*

496 *Buergerianum. Shandong Forestry Science and Technology* **48(04)**: 1-5.

497

498 **Allario T, Brumos J, Colmenero-Flores JM, Tadeo F, Morillon, R. 2011.** Large changes in

499 anatomy and physiology between diploid rangpur lime (*Citrus limonia*) and its autotetraploid are

500 not associated with large changes in leaf gene expression. *Journal of Experimental Botany*

501 62(8):2507-2519. https://doi.org/10.1093/jxb/erq467

502

503 **Allen JF, Forsberg J. 2001.** Molecular recognition in thylakoid structure and function. **6(7)**: 0-

504 326. DOI: 10.1016/S1360-1385(01)02010-6

505

506 **Arnon DI. 1949.** Copper enzymes in isolated chloroplasts. Polyphenoloxidase in beta-vulgaris.

507 Plant Physiol 24: 1-15.

508 DOI: 10.1104/pp.24.1.1

509

510 **Beale S. 2005.** Green genes gleaned. *Trends in Plant Science* **10(7)**:309-312.

511 DOI: 10.1016/j.tplants.2005.05.005

512

513 **Chen YG, Chen JF, Li WG, Cui L, Chen LZ. 2010.** Photosynthetic characteristics and

514 ultrastructure in *Cucumis* allopolyploids with different ploid levels. *Journal of Nanjing*

515 *Agriculturel University* **33(01)**:32-36.

516

517 **Chinese Flora Editorial Board of the Chinese Academy of Sciences. 1981.** *Chinese flora*.Vol.

518 46. Beijing: Science Press, 183.

519

Coate JE, Schlueter JA, Whaley AM, Doyle JJ. 2014. Divergent evolutionary fates of major photosynthetic gene networks following gene and whole genome duplications. *Plant Signal Behav* **6(4):**2081-2095. DOI: 10.4161/psb.6.4.15370

Coate JE, Luciano AK, Seralathan V, Minchew KJ, Owens TG, Doyle JJ. 2012. Anatomical, biochemical, and photosynthetic responses to recent allopolyploidy in *Glycine dolichocarpa* (Fabaceae). *American Journal of Botany* **99**: 55-67. DOI: 10.3732/ajb.1100465

Cock PJA, Fields CJ, Naohisa G, Heuer ML, Rice PM. 2010. The sanger fastq file format for sequences with quality scores, and the solexa/illumina fastq variants. *Nucleic Acids Research* **6(38)**:1767-1771. https://doi.org/10.1093/nar/gkp1137

Comai L. 2005. The advantages and disadvantages of being polyploid. *Nature Reviews Genetics* **6**: 836-846. DOI: https://doi.org/10.1038/nrg1711

Conesa A, Götz S, García-Gómez JM, Terol J, Talón M, Robles M. 2005. Blast2GO: Auniversal tool for annotation, visualization and analysis in functional genomics research. *Bioinformatics* **21**: 3674-3676.

Dhooghe E, Laere KV, Eeckhaut T Leus L, Huylenbroeck J. 2011. Mitotic chromosome doubling of plant tissues in vitro. *Plant Cell Tissue & Organ Culture* **104(3)**:359-373. DOI: 10.1007/s11240-010-9786-5

Dong B, Wang HB, Liu T, Cheng PL, Chen Y, Chen SM, Guan ZY, Fang WM, Jiang JF, Chen FD. 2017. Whole genome duplication enhances the photosynthetic capacity of *Chrysanthemum nankingense. Molecular Genetics and Genomics* **292**: 1247-1256. DOI: 10.1007/s00438-017-1344-y

See above.

547

Doležel J, Greilhuber J, Suda J. 2007. Estimation of nuclear DNA content in plants using flow

cytometry. *Nature Protocols* **2(9)**: 2233-2244.

DOI: https://doi.org/10.1038/nprot.2007.310

551

Du L, Li YC, Mu HZ, Zhang TY, Liu FF, Huang HJ, Liu GF. 2011. Photosynthetic

Characteristics of Tetraploid and Diploid *Betula platyphylla. Journal of Northeast Forestry*

University **39 (2):** 1-4. DOI:10.13759/j.cnki.dlxb.2011.02.017

555

Eckhardt U, Grimm B, Hörtensteiner S. 2004. Recent advances in chlorophyll biosynthesis

and breakdown in higher plants. *Plant Mol. Biol* 56: 1-14. DOI: 10.1007/s11103-004-2331-3

558

Edger PP, Pires JC. 2009. Gene and genome duplications: the impact of dosage-sensitivity on

the fate of nuclear genes. *Chromosome Res* **17(5):** 699-717.

DOI: 10.1007/s10577-009-9055-9

562

Evans JR. 2013. Improving photosynthesis. *Plant Physiol* **162**: 1780-1793.

DOI: 10.1104/pp.113.219006

565

Falbel TG, Staehelin LA. 2008. Partial blocks in the early steps of the chlorophyll synthesis

pathway: A common feature of chlorophyll b-deficient mutants. *Physiologia Plantarum*

97(2):311-320. DOI: 10.1034/j.1399-3054.1996.970214.x

569

Feng YZ, Chen HY, Yu TY, Feng QD. 2012. Research Progress on Acid Deposition over

China and Effect of Acid Rain on Agricultural Production. *Chinese Agricultural Science Bulletin*

28(11):306-311.

573

574 **Gao S, Yan Q, Chen L, Song Y, Li J, Fu C, Dong M. 2017.** Effects of ploidy level

575 and haplotype on variation of photosynthetic traits: novel evidence from two *Fragaria*

576 species. *PLoS One* **12**: e0179899. DOI: 10.1371/journal.pone.0179899

577

578 **Grabherr MG, Haas BJ, Yassour M, Levin JZ, Thompson DA, Amit I, Adiconis X, Fan L,**

579 **Raychowdhury R, Zeng Q. 2011.** Full-length transcriptome assembly from RNA-Seq data

580 without a reference genome. *Nat. Biotechnol* 29 644-652.

581 DOI: https://doi.org/10.1038/nbt.1883

582

583 **Greenwood AD, Leech RM, Williams JP. 1963.** The osmiophilic globules of chloroplasts. I.

584 Osmiophilic globules as a normal component of chloroplasts and their isolation and composition

585 in *Vicia faba* L. *Biochimica Et Biophysica Acta* **78(1):**148-162.

586 DOI: 10.1016/0006-3002(63)91620-2

587

588 **Guo X, Guo WH, Luo YJ, Tan XF, Du N, Wang RQ. 2013.** Morphological and biomass

589 characteristic acclimation of trident maple (*Acer buergerianum* Miq.) in response to light and

590 water stress. *Acta Physiologiae Plantarum* **35(4)**:1149-1159.

591 DOI: 10.1007/s11738-012-1154-0

592

593 **Hayashi M. 2007.** Tree bark handbook. Tokyo: Bun-ichi Co.Ltd.

594

595 **Kanehisa M, Araki M, Goto S, Hattori M, Hirakawa M, Itoh M, Katayama T, Kawashima**

596 **S, Okuda S, Tokimatsu T. 2008.** KEGG for linking genomes to life and the environment.

597 *Nucleic Acids Res* **36**: D480-D484.

598

599 **Kramer DM, Johnson G, Kiirats O, Edwards GE. 2004.** New fluorescence parameters

600 for the determination of QA redox state and excitation energy fluxes. *Photosynth.*

601   *Res* **79:** 209-218. DOI: 10.1023/B:PRES.0000015391.99477.0d

602

603   **Kron P, Husband BC. 2012.** Using flow cytometry to estimate pollen DNA content: improved

604   methodology and applications. *Ann BotLondon* **110(5)**: 1067-1078.

605   DOI: 10.1093/aob/mcs167

606

607   **Leal-Bertioli SC, Moretzsohn MC, Santos SP, Brasileiro AC, Guimaraes PM, Bertioli DJ,**

608   **Araujo AC. 2017.** Phenotypic effects of allotetraploidization of wild Arachis and their

609   implications for peanut domestication. *American Journal of Botany* **104**: 379-388.

610   DOI: 10.3732/ajb.1600402

611

612   **Liang HZ, Dou DQ, Feng YL. 2004.** Diurnal changes in photosynthesis and chlorophyll

613   fluorescence parameters of *Amoomvilosum* lour. *Acta Ecologica Sinica* **24(7):** 1421-1429.

614

615   **Li HS. 2000.** *Principles and techniques of plant physiological and biochemical experiments.*

616   Beijing: Higher Education Press. 134-138.

617

618   **Li W, Yang S, Lu Z, He Z, Ye Y, Zhao B, Wang L, Jin B. 2018.** Cytological, physiological,

619   and transcriptomic analyses of golden leaf coloration in *Ginkgo biloba* L. *Horticulture Research*

620   **5**: 12. https://doi.org/10.1038/s41438-018-0015-4

621

622   **Liu Y, Li X, Liu M, Cao B, Tan H, Wang J, Li X. 2012.** Responses of three different ecotypes

623   of reed (*Phragmites communis* Trin.) to their natural habitats: leaf surface micro-morphology,

624   anatomy, chloroplast ultrastructure and physio-chemical characteristics. *Plant Physiology &*

625   *Biochemistry* **51**: 159-167. DOI: 10.1016/j.plaphy.2011.11.002

626

627   **Masuda T, Fujita Y. 2008.** Regulation and evolution of chlorophyll metabolism. *Photochem.*

628   *Photobiol. Sci.* **7:** 1131-1149.

629

630   **Matsumoto M, Yada M, Hatakeyama S, Ishimoto H, Tanimura T, Tsuji S, Kakizuka A,**

631   **Kitagawa M, Nakayama KI. 2004.** Molecular clearance of ataxin-3 is regulated by a

632   mammalian E4. *Embo Journal* 23: 659-669.

633   DOI: 10.1038/sj.emboj.7600081

634

635   **Matsue M, Takeda Y. 2009.** Technical Note of National Institute for Land and Infrastructure

636   Management, No. 506. The Street Tree of Japan VI, National Institute for Land and

637   Infrastructure Management, Ministry of Land, Infrastructure, Transport, and Tourism; 76.

638

639   **Ohmiya A, Hirashima M, Yagi M, Tanase K, Yamamizo C. 2014.** Identification of Genes

640   Associated with Chlorophyll Accumulation in Flower Petals. *Plos One* **9(12)**: e113738.

641   DOI: 10.1371/journal.pone.0113738

642

643   **Otto SP. 2007.** The evolutionary consequences of polyploidy. *Cell* **131**: 452-462.

644   DOI: 10.1016/j.cell.2007.10.022

645

646   **Paul K, Husband BC. 2012.** Using flow cytometry to estimate pollen DNA content: improved

647   methodology and applications. *Annals of Botany* **(5)**:1067-1078. DOI: 10.1093/aob/mcs167

648

649   **Pertea G, Huang X, Liang F, Antonescu V, Sultana R, Karamycheva S, Lee Y, White J,**

650   **Cheung F, Parvizi B, Tsai J,Quackenbush J. 2003.** TIGR gene indices clustering tools

651   (TGICL): A software system for fast clustering of large EST datasets. *Bioinformatics* **19**: 651-

652   652. DOI: 10.1093/bioinformatics/btg034

653

654   **Tang W, Wang W, Chen D, Ji Q, Jing Y, Wang H, Lin R. 2012.** Transposase-derived proteins

655 FHY3/FAR1 interact with phytochrome interacting factor1 to regulate chlorophyll biosynthesis

656 by modulating HEMB1 during deetiolation in *Arabidopsis*. *Plant Cell*

657 2**4(5)**: 1984-2000. https ://doi.org/10.1105/tpc.112.09702 2

658

659 **Van Laere K, Franca SC, Vansteenkiste H, Van Huylenbroeck J, Steppe K, Van Labeke**

660 **MC. 2010.** Influence of ploidy level on morphology, growth and drought susceptibility in

661 *Spathiphyllum wallisii. Acta Physiologiae Plantarum* **33(4)**:1149-1156.

662 DOI: 10.1007/s11738-010-0643-2

663

664 **Wang BS, Han JF, Wang YL, Sui DZ. 2006.** A preliminary study on the seedling stage test of

665 several garden maples. *Journal of Jiangsu Forestry Science & Technology* **34 (1):** 10-14.

666

667 **Wang L, Feng Z, Wang X, Wang X, Zhang X. 2010.** Degseq: an R package for identifying

668 differentially expressed genes from rna-seq data. *Bioinformatics* **26(1)**:136-138.

669 https://doi.org/10.1093/bioinformatics/btp612

670

671 **Wang Y, Zhang XS, Deng MJ, Zhao ZL, Fan GQ. 2013.** Study on Photosynthetic

672 Characteristics of Diploid and Tetraploid *Paulownia australis*. *Acta Agriculturae Jiangxi*

673 **25(08)**: 39-42+45.

674

675 Wang Z. 2000. Plant Physiology. *Beijing: China Agriculture Press*. 125-128.

676

677 **Warner DA, Edwards GE. 1993.** Effects of polyploidy on photosynthesis. *Photosynth*

678 *Research* **35**: 135-147. DOI: 10.1007/BF00014744

679

680 **Xu Y. 1998.** The Systematic Evolution and Distribution of the Genus *Acer*. *ACTA*

681 *BOTANICA YUNNANICA* **20(4)**:383-393.

682

683 **Yamori W, Shikanai T. 2016.** Physiological functions of cyclic electron transport around

684 photosystem I in sustaining photosynthesis and plant growth. *Annual review of plant biology* 67:

685 81-106.

686 DOI: 10.1146/annurev-arplant-043015-112002

687

688 **Zhang F, Hu HQ, Wang LH, Zhou Q, Huang XH. 2018.** Effects of rare earth and acid rain

689 pollution on plant chloroplast ATP synthase and element contents at different growth stages.

690 *Chemosphere Oxford* **194**: 441-449. DOI: 10.1016/j.chemosphere.2017.12.001

691

692 **Zhang JE, Guo WW, Deng XX. 2006.** Relationship between ploidy variation of citrus calli and

693 competence for somatic embryogenesis. *Acta Genet. Sin.* 33: 647-654.

694 DOI: 10.1016/S0379-4172(06)60095-4

695

696 **Zhu HJ, Liu WG, Zhao SJ, Yan ZH, Lu XQ, He N, Yuan PL, Guan LY. 2012.** Leaf Ultra-

697 structure Comparison of Watermelon Seedling with Different Ploidy. *China Cucurbits and*

698 *Vegetables* **25(03)**: 5-7. DOI: 10.16861/j.cnki.zggc.2012.03.002

699

700 **Zhang YB, Chen JF, Yi HP, Feng JX, Wu MZ. 2005.** Staining and Slide-preparing Technique

701 of Mitotic Chromosomesand Its Use in Karyotype Determination of *Cucumis melo* L. *Acta*

702 *Botanica Boreali-Occidentalia Sinica* (09): 1735-1739.

Maximum gas exchange parameters of different ploidies

It contains the maximum values of T_r,P_n,C_i,G_s from May to September.

2   Table 1. Maximum gas exchange parameters of different ploidy

Month	Ploidy	Maximum net photosynthetic rate ($P_{n\ max}$, $\mu mol \cdot m^{-2} \cdot s^{-1}$)	Maximum stomatal conductance ($G_{s\ max}$, $mol \cdot m^{-2} \cdot s^{-1}$)	Maximum CO_2 concentration ($C_{i\ max}$, $\mu mol \cdot mol^{-1}$)	Maximum transpiration rate ($T_{r\ max}$, $mol \cdot m^{-2} \cdot s^{-1}$)
May	Tetraploid X	5.3227±0.116a	0.1192±0.010a	309.7800±5.34a	1.1123±0.128
	Diploid S	5.1029±0.020b	0.0864±0.004b	293.4500±3.83b	0.9872±0.036
June	Tetraploid X	5.9249±0.153a	0.1174±0.008a	351.7200±3.112a	1.2764±0.230
	Diploid S	5.2735±0.030b	0.0828±0.000b	301.0400±16.64b	1.0885±0.046
July	Tetraploid X	8.4846±0.179a	0.1123±0.006a	355.2300±8.338a	1.3319±0.110
	Diploid S	7.8211±0.029b	0.0907±0.000b	301.0400±16.64b	1.2282±0.006
August	Tetraploid X	11.1538±0.455a	0.1900±0.143a	335.2800±2.656a	1.1238±0.048
	Diploid S	8.5592±0.024b	0.1454±0.005b	301.4300±10.334b	0.8357±0.011
September	Tetraploid X	9.1703±0.180a	0.1448±0.006a	323.5100±6.417a	1.2562±0.030
	Diploid S	8.5103±0.032b	0.1189±0.004b	294.5100±11.461b	0.9756±0.014

5   Values represent the mean ± standard error (SE) of at least three tagged in dividuals of each ploidy type.

6   Different lowercase letters within a row indicate statistically significant differences ($P < 0.01$) between the two ploidy level on

7   the same day. The same letters mean the difference is not significant, and the different letters mean the difference is significant.

Differentially expressed genes in the chlorophyll synthesis pathway

It contains information about genename,geneID,and size.

Table 2. Differentially expressed genes in the chlorophyll synthesis pathway

Gene name	Gene ID	Size (bp)	log2 (X/S)
	CL3197.Contig1	1743	1.2136
	CL3197.Contig2	1848	4.9716
HemB	CL3197.Contig3	1474	1.8448
	CL3197.Contig4	1213	7.4426
	CL3197.Contig5	1343	7.2818
HemC	CL3343.Contig1	1446	-1.8068
HemE	CL633.Contig2	1641	-1.0693
	CL6001.Contig1	2592	-1.6240
CHLH/D/I	CL6001.Contig2	2776	3.7295
	Unigene11625	2263	-1.1987

Figure 1

Chlorophyll contents and chlorophyll fluorescence parameters in X and S

The leaf chlorophyll a/b content and chlorophyll fluorescence parameters in X and S. Asterisk mean values for the X and S differ signifcantly according to ANOVA (p < 0.05).

A

Chlorophyll contents in X and S

B

Chlorophyll fluorescence parameters in X and S
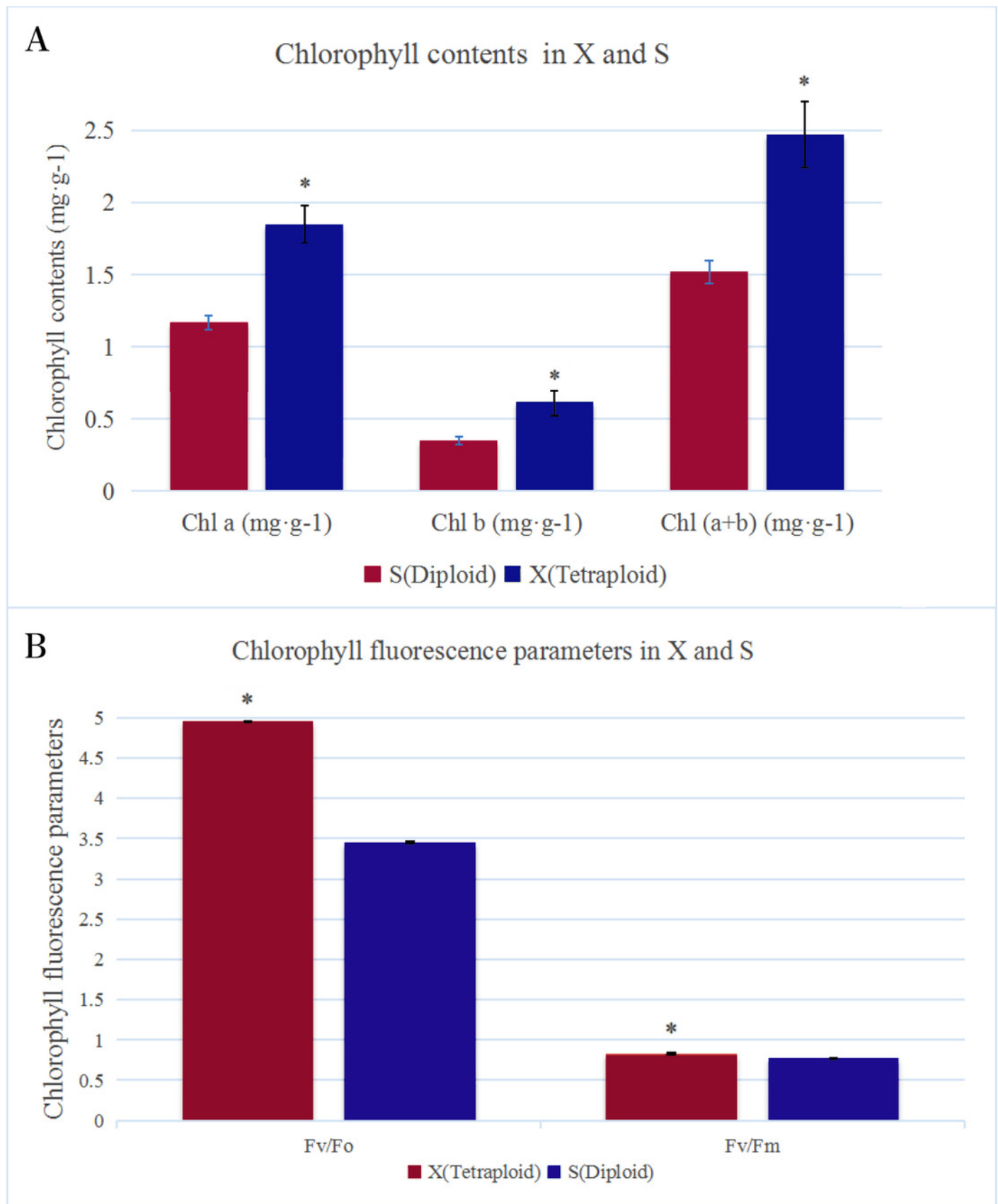
Figure 2

Ultrastructure of the mesophyll cell chloroplasts

A and a: A. buergerianum diploid; B and b: A. buergerianum tetraploid. Ch: chloroplast; SG: starch grains; G: grana; O: plastoglobuli.
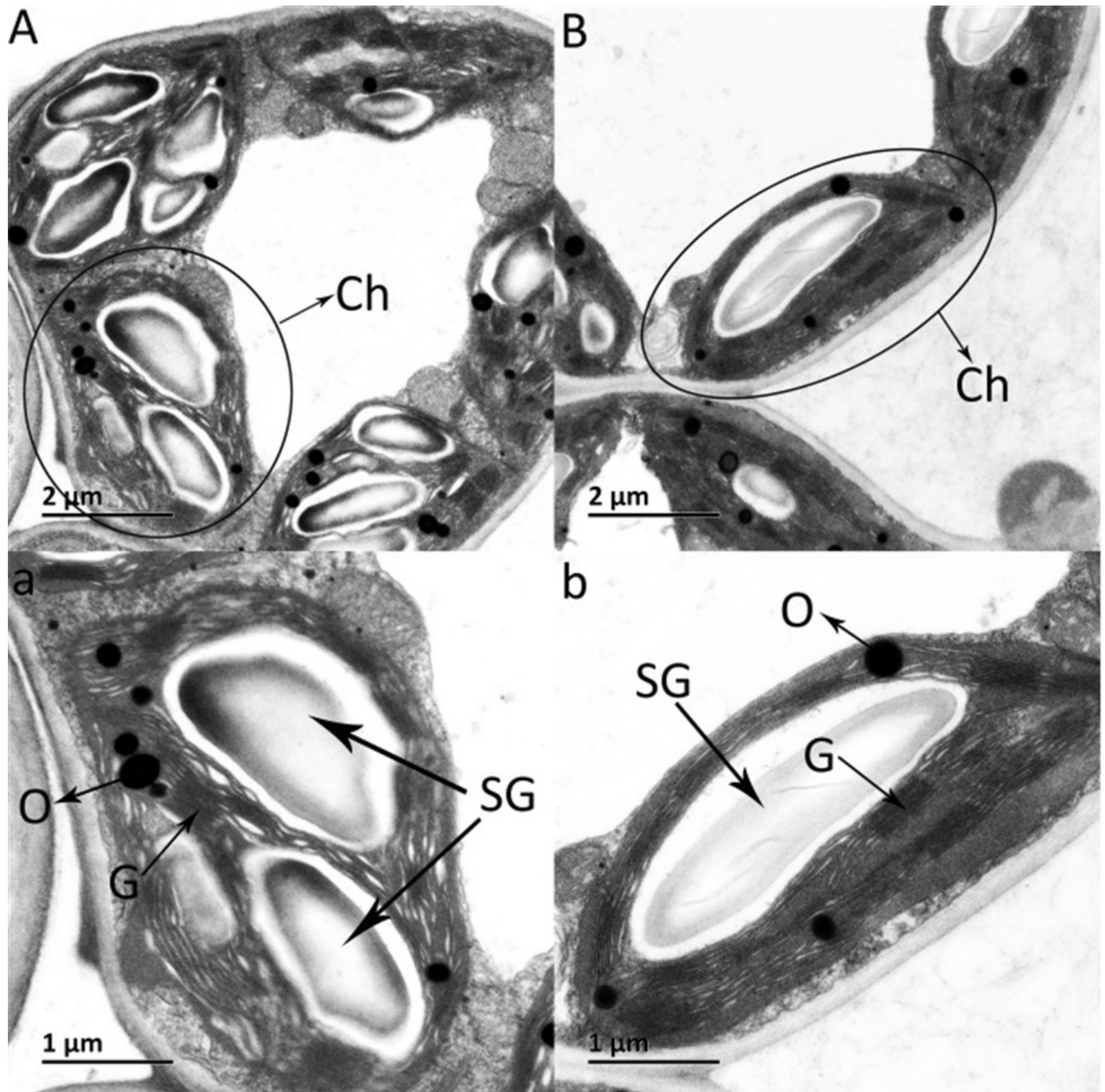
Figure 3

Comparison of thylakoid lamella thickness and plastoglobuli number of X and S
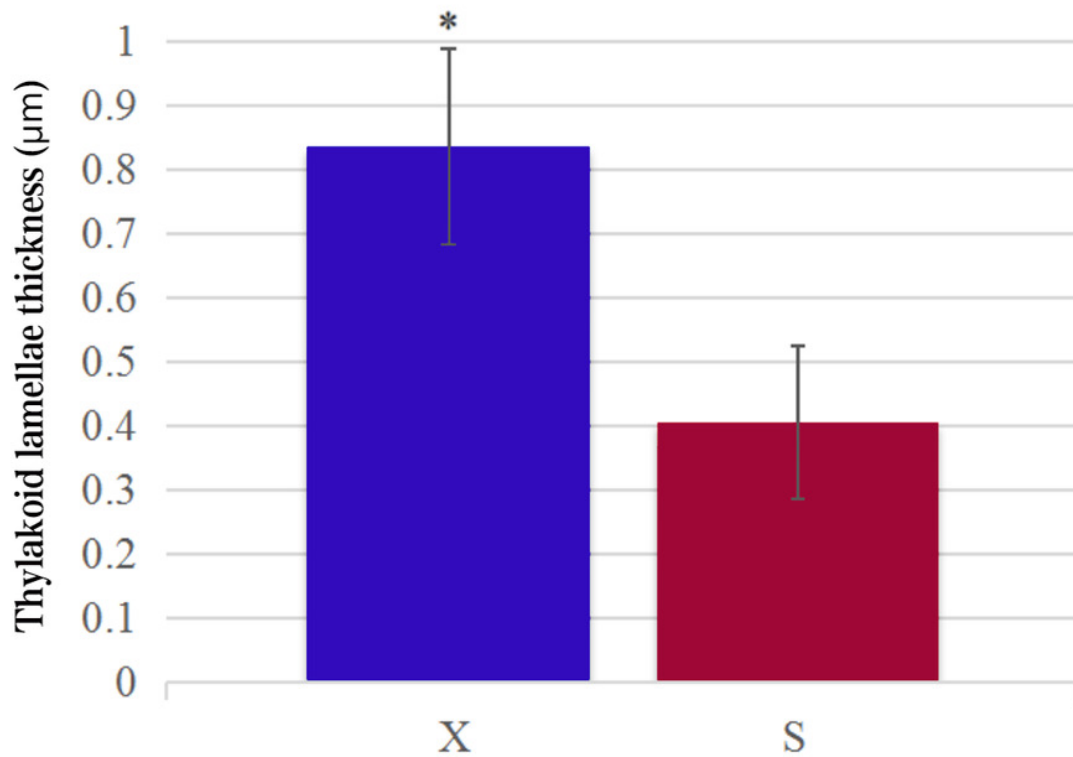
Asterisk mean values for the X and S differ signifcantly according to ANOVA (p < 0.05).
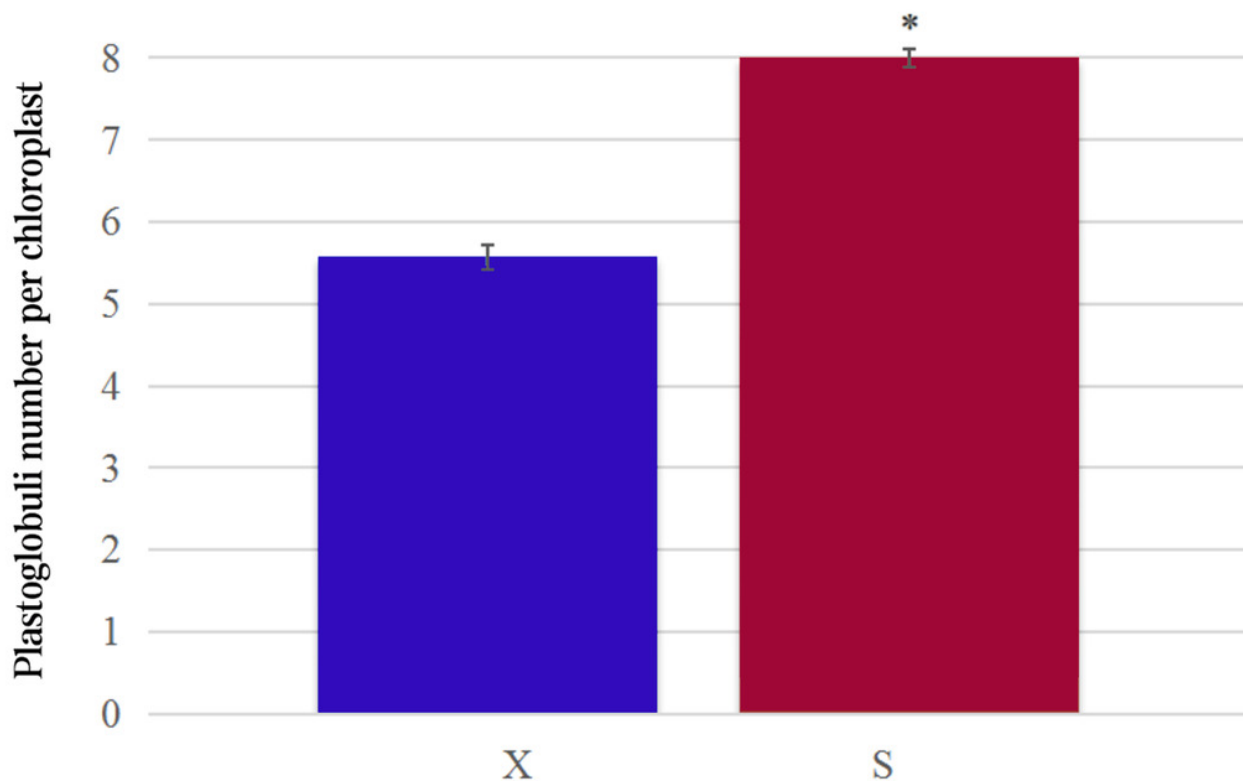
Figure 4

Photosynthesis pathway

Up-regulated genes in *A. buergerianum* X are represented by purple boxes, and down-regulated genes are represented by blue boxes.

Figure 5

Schematic diagram for the possible mechanisms for the increased photosynthetic capacity of X